ESC HEART FAILURE
ESC Heart Failure 2021; **8**: 280–290
Published online 19 November 2020 in Wiley Online Library (wileyonlinelibrary.com) **DOI:** 10.1002/ehf2.13037

ORIGINAL RESEARCH ARTICLE

Comprehensive plasma metabolites profiling reveals phosphatidylcholine species as potential predictors for cardiac resynchronization therapy response

Shengwen Yang[1,2], Yiran Hu[1], Junhan Zhao[1], Ran Jing[1], Jing Wang[1], Min Gu[1], Hongxia Niu[1], Liang Chen[1,3]* and Wei Hua[1]*

[1]*Arrhythmia Center, State Key Laboratory of Cardiovascular Disease, Fuwai Hospital, National Center for Cardiovascular Diseases, Chinese Academy of Medical Sciences and Peking Union Medical College, No. 167 Beilishi Road, Xicheng District, Beijing, 100037, China;* [2]*Heart Center & Beijing Key Laboratory of Hypertension, Beijing Chaoyang Hospital, Capital Medical University, Beijing, 100020, China;* [3]*Department of cardiac surgery,State Key Laboratory of Cardiovascular Disease, Fuwai Hospital, National Center for Cardiovascular Diseases, Chinese Academy of Medical Sciences and Peking Union Medical College, No. 167 Beilishi Road, Xicheng District, Beijing, 100037, China*

Abstract

Aims This study aimed to identify the plasma metabolite fingerprint in patients with heart failure and to develop a prediction tool based on differential metabolites for predicting the response to cardiac resynchronization therapy (CRT).

Methods and results We prospectively recruited 32 healthy individuals and 42 consecutive patients with HF who underwent CRT between January 2018 and January 2019. Peripheral venous blood samples, clinical data, and echocardiographic signatures were collected before CRT implantation. Liquid chromatography-mass spectrometry was used to perform untargeted metabolites profiling for peripheral plasma under ESI+ and ESI− modes. After 6 month follow-up, patients were categorized as CRT responders or non-responders based on the alterations of echocardiographic characteristics. Compared with healthy individuals, patients with HF had distinct metabolomic profiles under both ESI+ and ESI− modes, featuring increased free fatty acids, carnitine, β-hydroxybutyrate, and dysregulated lipids with heterogeneous alterations such as phosphatidylcholines (PCs) and sphingomyelins. Disparities of baseline metabolomics profile were observed between CRT responders and non-responders under ESI+ mode but not under ESI− mode. Further metabolites analysis revealed that a group of 20 PCs metabolites under ESI+ mode were major contributors to the distinct profiles between the two groups. We utilized LASSO regression model and identified a panel of four PCs metabolites [including PC (20:0/18:4), PC (20:4/20:0), PC 40:4, and PC (20:4/18:0)] as major predictors for CRT response prediction. Among our whole population (n = 42), receive operating characteristics analysis revealed that the four PCs-based model could nicely discriminate the CRT responders from non-responders (area under the curve = 0.906) with a sensitivity of 83.3% and a specificity of 90.0%. Cross-validation analysis also showed a satisfactory and robust performance of the model with the area under the curve of 0.910 in the training dataset and 0.880 in the testing dataset.

Conclusions Patients with HF held significantly altered plasma metabolomics profile compared with the healthy individuals. Within the HF group, the non-responders had a distinct plasma metabolomics profile in contrast to the responders to CRT, which was characterized by increased PCs species. A novel predictive model incorporating four PCs metabolites performed well in identifying CRT non-responders. These four PCs might severe as potential biomarkers for predicting CRT response. Further validations are needed in multi-centre studies with larger external cohorts.

Keywords Cardiac resynchronization therapy; Metabolomics; Heart failure; Prediction

Received: 9 March 2020; Revised: 6 July 2020; Accepted: 15 September 2020
**Correspondence to: Wei Hua and Liang Chen, Arrhythmia Center, State Key Laboratory of Cardiovascular Disease, Fuwai Hospital, National Center for Cardiovascular Diseases, Chinese Academy of Medical Sciences and Peking Union Medical College, No. 167 Beilishi Road, Xicheng District, Beijing 100037, China. Phone: +86-3801134270; Fax: +86-68334688.*
Email: drhuaweifw@sina.com; liang.chen9@hotmail.com
Shengwen Yang, Yiran Hu, and Junhan Zhao, These authors contributed equally to this work.

Introduction

Heart failure (HF), a leading cause of substantial morbidity and mortality, affects about 2% of the adult population worldwide.[1] As a complex clinical syndrome, HF is associated with ventricular desynchrony and energy system abnormalities.[2–4] Cardiac resynchronization therapy (CRT) is an efficient treatment for patients with drug-refractory HF, which enables an improvement in both heart function and quality of life and prolongs survival time.[5–9] Although some patients meet with the latest criteria for implantation, in fact, up to 30% of them may not benefit from CRT.[10,11] It remains a challenge for clinicians to identify high-risk patients with poor outcomes before device implantation.

Metabolomics is defined as the comprehensive analysis of the metabolome of the biological system under defined conditions, reflecting the biochemical reaction.[12,13] As the systematic analysis of small-molecule metabolites, it provides the fingerprint of phenotypic alterations in pathophysiological states. Through the high-throughput technique by liquid chromatography-mass spectrometry (LC-MS/MS), it is possible to identify biomarkers in response to particular pathophysiological changes and explore their correlation to clinical phenotypes of diseases. Recent studies have demonstrated that metabolic alterations in patients with HF can be used as predictors for risk stratification.[14,15] Yet scarce information is available regarding the relationship between metabolites and response of CRT in patients with HF.

The purposes of this prospective study were (1) to assess the specific metabolic profiles of patients with HF compared with healthy individuals; (2) to investigate whether metabolic profiles show differences between CRT responders and non-responders; (3) to develop an applicable predictor with predictive metabolites for evaluating CRT response in patients with HF.

Methods

Study population

We prospectively recruited 42 consecutive patients with HF who had undergone CRT device implantation with defibrillator or not between January 2018 and January 2019 in Fuwai Hospital, Beijing, China. Before device implantation, all patients had received optimal medical therapy for at least 6 months. Inclusion criteria were New York Heart Association II-IV functional class with left ventricular ejection fraction (LVEF) 35% or less and QRS duration more than 120 ms, which were in accordance with guidelines for cardiac resynchronization and defibrillation.[16] Exclusion criteria were clinical and haemodynamic instability, tumour with a life expectancy of <1 year, end-stage renal disease, and absence of blood samples. Thirty-two (age 42.0 ± 15.2 and 19 men) healthy participants were recruited as a control group. No documented cardiovascular diseases or history of cardiovascular medication were recorded in the control group.

The Institutional Review Board of our institution approved the protocol, which was in compliance with the Declaration of Helsinki. All participants fully understood the details of the study and provided written informed consent.

Study protocol

All patients underwent clinical and physical examinations. Clinical characteristics were obtained from the electronic health records. All devices were implanted through the cephalic or subclavian left vein into the right atrium, the apex of the right ventricular, and the coronary sinus to pace the left ventricle and into the coronary sinus to pace the left ventricle lateral wall. Transthoracic echocardiography was performed according to the American Society of Echocardiography guidelines,[17] and left ventricular end-diastolic diameter and LVEF were measured by using biplane Simpson's method. Echocardiographic signatures were measured by two-dimensional echocardiography (Vivid 7 Dimension/Pro System, GE Healthcare, USA). According to the findings of clinical and echocardiographic alterations after 6 month follow-up, patients were categorized into two groups. Responders were defined as patients with an increase of LVEF more than 5% after CRT implantation. Non-responders were defined as patients with unchanged LVEF or an increase of $<5\%$ or who has been hospitalized or had undergone cardiac transplantation or had died due to worsening HF after CRT implantation.[18,19]

Blood samples collection and sample preparations for metabolomics

Peripheral venous blood samples were drawn from the cubital vein in the fasting state in the morning. For patients, blood samples were collected 1 day before the CRT implantation. Blood samples were stored in ethylene diamine tetraacetie acid vacutainer tubes (BD Vacutainer, Franklin Lakes, NJ, USA) and then centrifuged at 3000 certrifugal force in g for 15 min at 4°C. Plasma was immediately separated and stored at −80°C until use.

The sample preparation for untargeted metabolomics was according to the manufacturer's instructions. To precipitate the protein, 400 μL of cold methanol was added to 100 μL of the plasma sample, vortexed for 60 s, and then were centrifuged at 14 000 *g* for 15 min. The supernatant was prepared for LC-MS/MS. Quality control (QC) samples were prepared by mixing equal volumes of each plasma sample.

The quality control sample was periodically injected with batches of 10 test samples throughout the analytical run.

Metabolomics data collection and analysis

A Dionex Ultimate 3000 RS UHPLC system (Thermo Fisher Scientific, Waltham, MA, USA) was equipped with ACQUITY UPLC BEH C8 column (1.7 μm, 2.1 × 100 mm, Waters Corp, Milford, USA) in positive mode and ACQUITY UPLC BEH C8 column (1.7 μm, 2.1 × 100 mm, Waters Corp, Milford, USA) and UPLC HSS T3 column (2.1 mm × 100 mm, 1.8 μm, Waters Corp, Milford, USA) in negative mode. In positive mode analysis, the binary gradient elution system consisted of (A) water (containing 0.1% formic acid, v/v) and (B) acetonitrile (containing 0.1% formic acid, v/v), and separation was achieved using the following gradient: 5–100% B over 0–24 min, the composition was held at 100% B at 24.1–27.5 min, then 27.5–27.6 min, 100% to 5% B, and 27.6–30 min holding at 5% B. In negative mode analysis, the binary gradient elution system consisted of (A) water (containing 6.5 mM ammonium acetate) and (B) 95% methanol (containing 6.5 mM ammonium acetate), and separation was achieved using the following gradient: 5–100% B over 1–18 min, the composition was held at 100% B at 18.1–22 min, then 22–22.1 min, 100% to 5% B, and 22.1–25 min holding at 5% B. The flow rate was 0.35 mL/min, and the column temperature was 50°C. All the samples were kept at 4°C during the analysis. The injection volume was 5 μL.

Mass spectrometry analysis was performed on a Q-Exactive quadrupole-Orbitrap mass spectrometer equipped with heated electrospray ionization (ESI) source (Thermo Fisher Scientific, Waltham, MA, USA) in both positive and negative ion modes. The mass range was from m/z 70 to 1000. The resolution was set at 70 000 for the full MS scans and 17 500 for HCD MS/MS scans. The collision energy was set at 10, 20, and 40 eV. The mass spectrometer operated as follows: spray voltage, 3800 V (positive) and 3000 V (negative); sheath gas flow rate, 35 arbitrary units; auxiliary gas flowrate, 8 arbitrary units; capillary temperature, 350°C.

Metabolomics data were acquired using the XCMS software (1.50.1 version), which produced a matrix of features with chromatography, accurate mass, and retention time. The variables presented in at least 50% of either group were extracted. All ions were normalized to the total peak area of each sample to achieve a minimum relative standard deviation (SD). Principle component analysis (PCA) and partial least-squares discriminant analysis (PLS-DA) were performed to identify the discrimination of variables. Benjamini–Hochberg false discovery rate procedure was employed for the multiple test adjustments. Adjusted P-values <0.05 were considered statistically significant. Differential metabolites were defined as those with variable importance in the projection (VIP) > 1.0 obtained from PLS-DA and adjusted P-values <0.05. VIP indicates the contribution of each variable to group differences. Heatmaps were obtained based on Spearman correlation and cluster analyses. The significant metabolites were identified by MS/MS fragment through OSI-SMMS (version 1.0, Dalian Chem Data Solution Information Technology Co. Ltd.) with an in-house MS/MS database. MetaboAnalyst 4.0 was used to identify a variety of functional enrichment analyses.

Statistical analysis

Clinical and echocardiographic characteristics were expressed as the mean ± SD for continuous variables and as the number (per cent) for categorical variables. The intensity of metabolites was expressed as median (IQR). Continuous variables of two groups were compared using the Student's t-test (for normally distributed) and the Wilcoxon test (for non-normally distributed and all metabolites). Categorical variables were compared by the χ^2 test or Fisher's exact test as appropriate. For the prediction model of CRT response, the least absolute shrinkage and selection operator (LASSO) was used to determine non-zero coefficient features, which were considered as the most important predictors. The tuning parameter (λ) was selected in the LASSO model used 10-fold cross-validation via minimum criteria and the 1 standard error (1-SE). And the model at 1-SE criteria was selected as the final model. The regression model was established by multivariable logistic regression. The performance of the prediction accuracy assessment was conducted by a receiver operating characteristic (ROC) curve with area under curve (AUC). Probability values were yielded from the prediction models, which were subsequently utilized as new input variables for the ROC curve analysis. The optimal cut-off value, which combined the higher value of specifying plus sensitivity, was identified from the ROC curve. A two-sided P value <0.05 was accepted as statistical significance. All data were analysed using the R Programming Language (version 3.3.1; https://www.r-project.org/).

Results

Baseline characteristics

In this study, a total of 42 HF patients who were scheduled for CRT implantation and 32 healthy subjects were included as the HF group and the control group, respectively. Clinical and echocardiographic characteristics of 30 CRT responders and 12 non-responders are presented in *Table 1*. Age and gender were comparable between the CRT responders and non-responders. The mean left ventricular end-diastolic diameter was 64.7 ± 7.9 mm in the CRT responders group and 71.9 ± 9.6 mm in the CRT non-responders group

Table 1 Demographics, clinical, and echocardiographic characteristics of cardiac resynchronization therapy responders versus non-responders at baseline

Variable	Responders (N = 27)	Non-responders (N = 11)	P value
Baseline			
Age, years	58.9 ± 10.6	57.0 ± 14.4	0.565
Gender, male	17 (63%)	8 (73%)	0.714
BMI, kg/m^2	26.4 ± 3.3	25.3 ± 3.2	0.430
Device type, CRT-D	9 (33%)	7 (64%)	0.086
SBP, mmHg	126.3 ± 20.9	113.9 ± 11.8	0.075
DBP, mmHg	72.2 ± 10.7	67.6 ± 7.0	0.201
HR, b.p.m.	71.5 ± 9.7	69.4 ± 10.4	0.562
NYHA functional class	2.5 ± 0.8	2.4 ± 0.7	0.577
Alcohol	7 (26%)	3 (27%)	0.932
Smoking	11 (41%)	3 (27%)	0.435
Co-morbidity			
Coronary artery disease	8 (30%)	2 (18%)	0.467
Hypertension	16 (59%)	1 (9%)	0.005
LBBB	23 (85%)	11 (100%)	0.177
Diabetes	12 (44%)	2 (18.2%)	0.128
Atrial fibrillation	2 (7%)	0 (0%)	0.354
Serum biomarkers			
Scr, μmol/L	88.4 ± 16.2	80.2 ± 16.6	0.181
hs-CRP, mg/L	2.8 ± 2.8	1.9 ± 1.8	0.354
NT-proBNP, pg/mL	1393.0 ± 1743.0	851.6 ± 891.4	0.337
Uric acid, μmol/L	392.9 ± 141.3	368.8 ± 155.1	0.663
Albumin, g/L	42.7 ± 5.1	43.2 ± 4.7	0.776
CK-MB, U/L	14.8 ± 12.5	12.6 ± 3.2	0.583
Medication			
ACEI/ARBs	24 (89%)	11 (100%)	0.249
Beta-blockers	25 (93%)	10 (91%)	0.861
Spironolactone	26 (96%)	9 (82%)	0.133
Trimetazidine	4 (15%)	5 (45%)	0.044
Amiodarone	3 (11%)	2 (18%)	0.559
Echocardiography			
LVEDD, mm	64.7 ± 7.9	71.9 ± 9.6	0.026
LVEF, %	35.5 ± 10.0	31.5 ± 8.5	0.243
Lad, mm	42.7 ± 5.5	43.1 ± 8.3	0.854

ACEI-ARBs, angiotensin-converting enzyme-angiotensin receptor blocker; BMI, body mass index; CK-MB, creatine kinase isoenzyme-MB; CRT-D, CRT device implantation with defibrillator; DBP, diastolic blood pressure; HR, heart rate; hs-CRP, high sensitivity C-reactive protein; LVEDD, left ventricular end-diastolic diameter; LVEF, left ventricular ejection fraction; NT-proBNP, N-terminal pro-brain natriuretic peptide; NYHA, New York Heart Association; SBP, systolic blood pressure.

(P = 0.026). In addition, compared with non-responders, the incidences of hypertension were higher among CRT responders (57% vs. 8%, P = 0.003). Furthermore, no significant differences between these two groups were observed in HF-related biomarkers such as N-terminal pro-brain natriuretic peptide, creatine, high sensitivity C-reactive protein, and creatine kinase isoenzyme-MB (CK-MB). And all the patients received conventional medication for HF, and drug treatment was similar between responders and non-responders, except for trimetazidine (13% vs. 50%, P = 0.014).

Metabolomics distinctions between the heart failure group and control group

We first evaluated the metabolic signatures between HF and control groups under either ESI+ or ESI− modes of untargeted metabolomics. Obtained by ESI+ metabolome, significant disparities were illustrated between patients with HF and healthy individuals through PCA plot and PLS-DA plot (*Figure 1A* and *B*). In the PLS-DA analysis, the cumulative R2Y and Q2 in the ESI+ mode were 0.991 and 0.882, respectively. There were 294 out of 982 metabolites (29.94%) in the ESI+ pattern metabolome showing VIP $>$ 1. Pronounced distinctions were also confirmed by PCA and PLS-DA under ESI− pattern as well (*Figure 1D* and *E*), in which the cumulative R2Y and Q2 were 0.981 and 0.847, respectively. Three hundred sixty-one out of 1386 metabolites (26.05%) in the ESI− pattern metabolome had VIP $>$ 1. For visualizing the relationship between the altered metabolites, hierarchical clustering with heatmap was used to arrange the metabolites based on their relative levels across samples as shown in *Figure 1C* (for ESI+) and *Figure 1F* (for ESI−). Overall, the metabolic signatures were significantly distinct between HF and control groups identified by either ESI+ or ESI− modes of LC-MS/MS.

Consistent with previous reports,[20–22] the untargeted plasma metabolome could significantly discriminate patients with HF from healthy individuals, independent of ESI positive or negative pattern. Compared with healthy individuals, patients with HF showed increased concentration of

FIGURE 1 Metabolite fingerprint between heart failure and healthy individuals. The unsupervised PCA (A) and three dimensions (3D) PLS-DA analysis (B) of plasma metabolites from heart failure and healthy controls identified by untargeted metabolomics under ESI+ pattern. (C) The heatmap with h-clustering of metabolic features under ESI+ exhibits well discrimination between most heart failure and healthy controls. The unsupervised PCA (D) and 3D PLS-DA analysis (E) of plasma metabolites from heart failure and healthy controls identified by untargeted metabolomics under ESI− pattern. (F) The heatmap with h-clustering of metabolic features under ESI− exhibits well discrimination between most heart failure and healthy controls. Violin plot at ROC curve of two representative differential metabolites between heart failure and healthy controls from ESI+ mode: biopterin (VIP = 3.694, G) and acetylcarnitine (VIP = 3.635, H), and from ESI− mode: histidine (VIP = 2.472, I) and octasecenoic acid (VIP = 3.134, J). All four metabolites were shown with good discrimination by ROC (all $P < 0.0001$, AUC = 0.818–0.988, G–J).

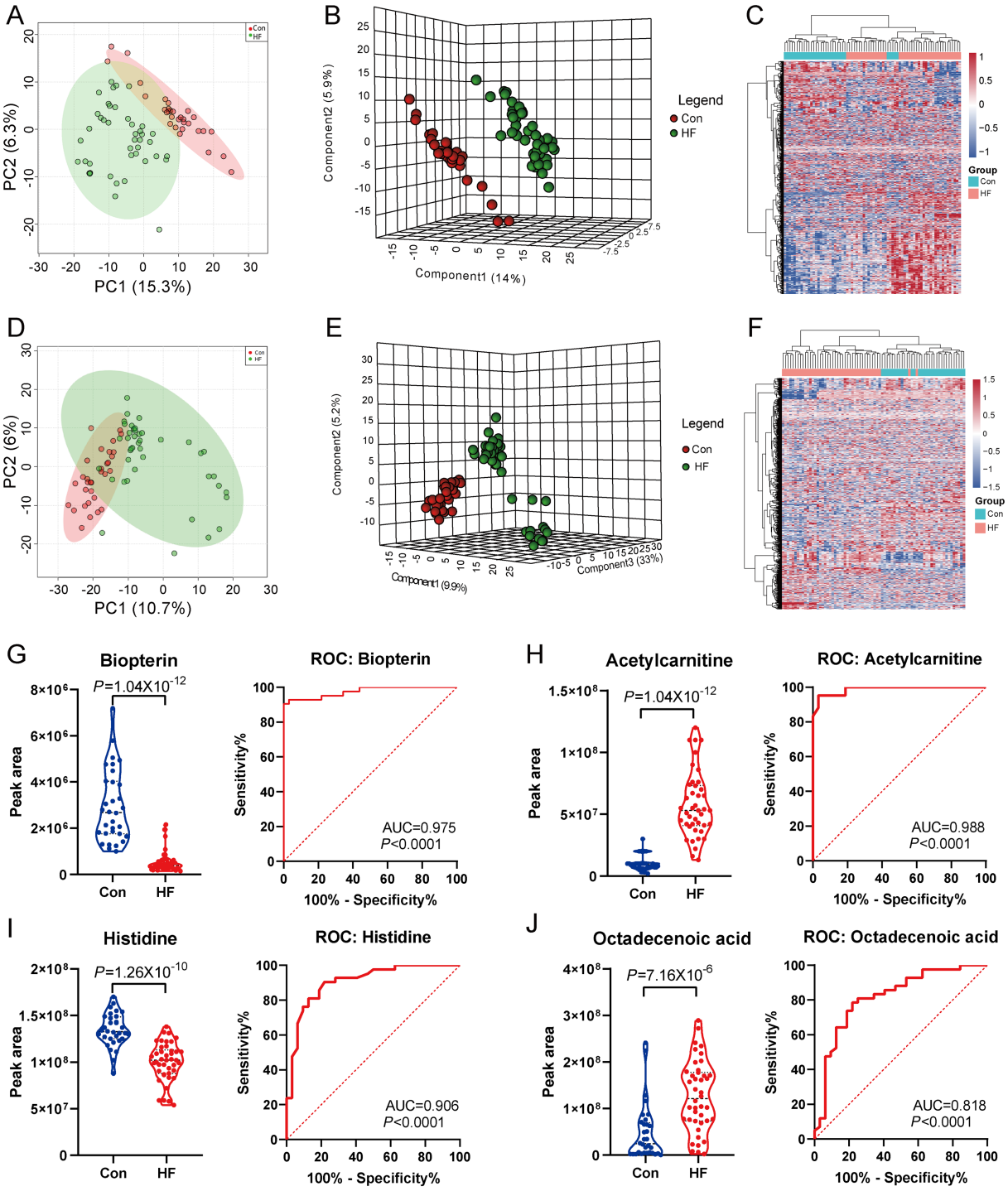

long-chain fatty acid, carnitine, β-hydroxybutyrate, and bilirubin. The lipid species, such as phosphatidylcholines (PCs) and sphingomyelins (SMs), exhibited heterogeneous alterations between HF and healthy individuals. Supporting Information *Table S1* presented the representative differential metabolites identified between HF patients and healthy controls (with VIP $>$ 2) via ESI+ and ESI− modes, respectively. Furthermore, we selected and plotted the top two metabolites between HF and control groups from ESI+ (biopterin and acetylcarnitine) and ESI− (histidine and octadecenoic acid) modes, respectively (*Figure 1G–J*). As shown by the ROC curve, the individual metabolite could discriminate against the HF and control individuals very well (all $P < 0.001$, AUC range: 0.818–0.988) (*Figure 1G–J*).

Discrimination of cardiac resynchronization therapy responders and cardiac resynchronization therapy non-responders

Obtained by ESI+ metabolome, significant disparity was illustrated between CRT responders and non-responders through PLS-DA (*Figure 2A*). The cumulative R2Y and Q2 were 0.858 and 0.591, respectively. However, the metabolic signatures under the ESI− pattern did not show significant difference between CRT responders and non-responders, as the cumulative R2Y and Q2 were 0.733 and −0.260, respectively (*Figure 2B*). Hence, we mainly focused on those metabolites detected by ESI+ pattern for further analysis. A total of 86 metabolites from in the ESI+ pattern metabolome with VIP $>$ 1 in the loading plot were highlighted as biomarker candidates in *Figure 2C*. Through the Mann–Whitney–Wilcoxon test with false discovery rate correction ($P < 0.05$), differential metabolic features were obtained and highlighted in *Figure 2D*. We combined the criteria of VIP $>$ 1.0 and $P < 0.05$ to further filter candidate metabolites. Among all the filtered differential metabolic features, a group of PCs species were identified as the top 20 differential variables (*Table 2*) and summarized as a heatmap (*Figure 2E*). All these 20 PCs were upregulated in the plasma of CRT non-responders compared with CRT responders, with fold change ranging from 1.17 to 1.83. Interestingly, 17 out of 20 PCs were also significantly increased in all these patients HF with CRT compared with healthy controls, except for PC 34:3 (POS_17552), PC 40:4 (POS_18822), and PC (20:5/18:1) (POS_18294). These results suggested that PCs, a sub-species of lipid, may play an essential role in discriminating the CRT response for patients with HF.

Moreover, we also analysed the differences between ceramide (Cer) and SMs species between CRT response and non-response patients (Supporting Information, *Table S2*). And it was not observed significant differences in most of these metabolites between these two groups.

Diagnostic potential of phosphatidylcholine species for cardiac resynchronization therapy response

To identify the key metabolites that were essential predictors of CRT response, we used LASSO logistic regression models and selected the optimal λ values at 1-SE criterion (*Figure 3A* and *B*). Based on this criterion, we identified four PC metabolites with non-zero coefficients from the 20 differential metabolites observed in the peripheral plasma between CRT responders and non-responders, namely, PC (20:0/18:4), PC (20:4/20:0), PC 40:4, and PC (20:4/18:0), respectively. Each of the four PC metabolites was found to be significant different between CRT responders and non-responders in the univariate analysis, including PC (20:0/18:4) [1.89 (1.56, 2.25) vs. 1.43 (1.20, 1.72), $P < 0.001$], PC (20:4/20:0) [2.62 (2.21, 3.62) vs. 1.94 (1.57, 2.28), $P < 0.001$], PC 40:4 [1.37 (1.06, 1.89) vs. 0.88 (0.69, 1.04), $P = 0.002$], and PC (20:4/18:0) [3.96 (3.16, 5.23) vs. 2.96 (2.38, 3.57), $P = 0.005$] (*Figure 3C*). We then established the logistic regression model with the combinations of these four biomarkers to predict the CRT response. We randomly split the dataset into training and testing cohort for 500 replications and performed the cross-validation. The median AUC of the ROC for discrimination of CRT response was 0.91 and 0.88 in the training and testing dataset, respectively (*Figure 3D*). Based on the whole population ($n = 42$), we plotted the ROC curve in predicting CRT response using the logistic regression model incorporating the four biomarkers. Using the optimal cut-off value of 0.275, this model could predict CRT response with a sensitivity and specificity of 83.3% and 90.0%, respectively (AUC = 0.906, $P < 0.001$, *Figure 3E*). Furthermore, compared with individual PC metabolite, the combination of four PCs had better discrimination performance for predicting CRT response according to the AUC of ROC (*Figure 3E*).

Discussion

Current guidelines recommend CRT implantation for a broad spectrum of patients with systolic dysfunction and wide QRS duration.[16] Still, approximately 30% of patients who meet with the implantation criteria failed to benefit from CRT devices.[10,11] Therefore, identifying the non-responders before implantation is urgently needed to avoid excessive treatment. Over the past few years, several studies have proposed multiple parameters to identify subsets of patients with poor prognosis, including clinical features, echocardiographic measurement, and laboratory biomarkers.[20–22] However, traditional predictors are unlikely to provide sufficient information for the prognosis of CRT.

Metabolomics can be used to show essential snapshots of pathophysiology mechanisms and may be used to develop

FIGURE 2 Comparison of metabolites fingerprints between CRT responders and non-responders. (A) Three dimension of PLS-DA plot present distinct metabolites fingerprints between CRT responders and non-responders under the ESI+ pattern. (B) Three dimension of PLS-DA plot showed non-significant discrimination of metabolites fingerprints between CRT responders and non-responders under the ESI− pattern. (C) The distribution of VIP of each metabolite under ESI+ pattern. VIP > 1 highlighted in red. (D) Volcano plot present the differential metabolites between response and non-response patients. (E) The heatmap of the median value of selected 20 differential metabolites (VIP > 1, $P < 0.05$) between CRT non-responders and responders.

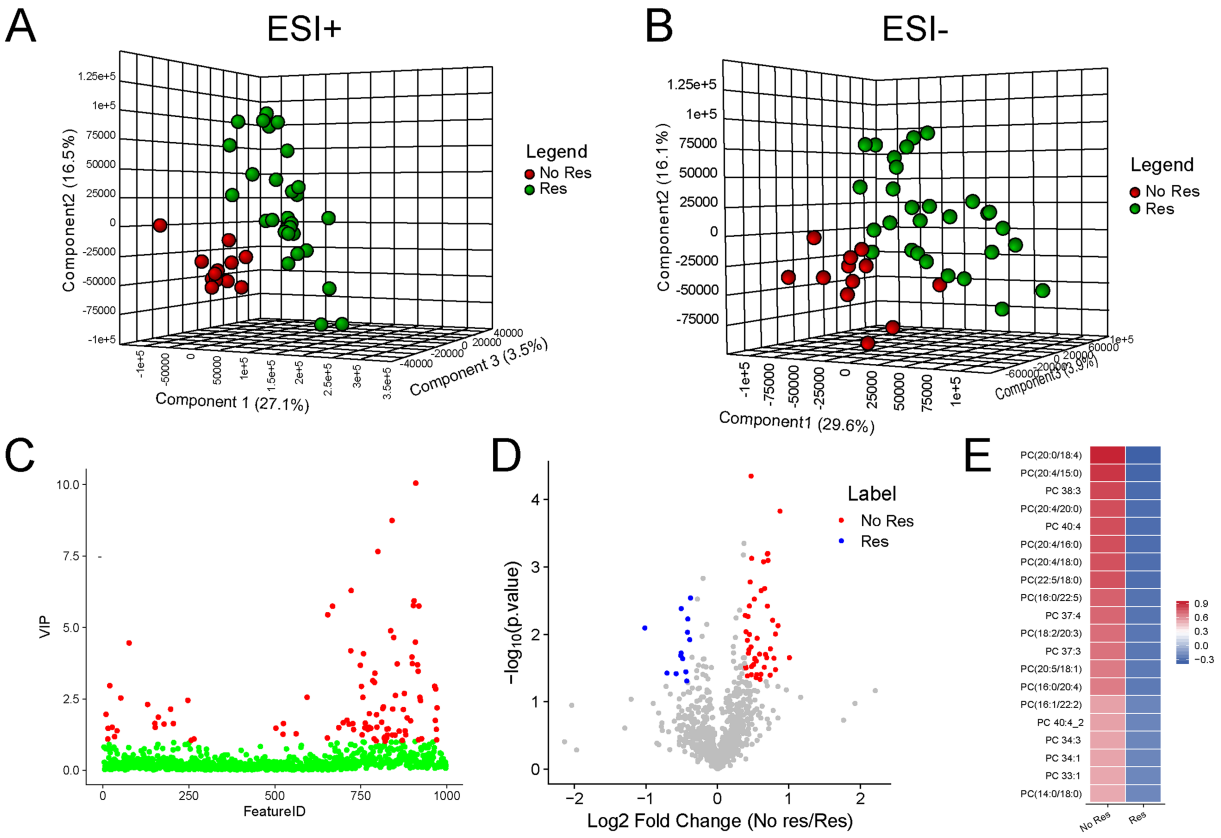

Table 2 Differential metabolites identified between cardiac resynchronization therapy response and non-response patients

Var ID	RT (min)	m/z	Metabolites	Formula	Fold	*P*	VIP	QC RSD
POS_18366	23.4135	810.5997	PC (20:0/18:4)	C46H84NO8P	1.38	0.0000	10.03	3.44
POS_17706	22.2982	768.5528	PC (20:4/15:0)	C43H78NO8P	1.83	0.0002	2.15	6.18
POS_18398	23.4129	812.6059	PC 38:3	C46H86NO8P	1.29	0.0005	3.45	3.28
POS_18820	23.6840	838.6237	PC (20:4/20:0)	C48H88NO8P	1.62	0.0006	1.42	10.63
POS_18822	24.0964	838.6311	PC 40:4	C48H88NO8P	1.62	0.0006	1.05	18.33
POS_17910	22.6954	782.5683	PC (20:4/16:0)	C44H80NO8P	1.28	0.0007	8.73	2.28
POS_18365	23.1496	810.5993	PC (20:4/18:0)	C46H84NO8P	1.39	0.0008	4.47	6.27
POS_18797	23.6858	836.6153	PC (22:5/18:0)	C48H86NO8P	1.63	0.0008	2.83	6.09
POS_18325	22.8768	808.5824	PC (16:0/22:5)	C46H82NO8P	1.37	0.0017	5.75	6.81
POS_18140	23.0570	796.5837	PC 37:4	C45H82NO8P	1.58	0.0021	2.68	5.68
POS_18327	22.8614	808.5843	PC (18:2/20:3)	C46H82NO8P	1.42	0.0030	5.92	7.45
POS_18177	23.3154	798.5987	PC 37:3	C45H84NO8P	1.36	0.0038	1.23	9.55
POS_18294	22.2896	806.5683	PC (20:5/18:1)	C46H80NO8P	1.34	0.0055	3.72	5.86
POS_17911	23.2830	782.5662	PC (16:0/20:4)	C44H80NO8P	1.19	0.0058	1.22	5.31
POS_18400	23.6559	812.6155	PC (16:1/22:2)	C46H86NO8P	1.28	0.0225	5.74	3.94
POS_18824	23.8753	838.6308	PC 40:4	C48H88NO8P	1.43	0.0229	2.17	7.14
POS_17552	21.8838	756.5438	PC 34:3	C42H78NO8P	1.45	0.0251	1.09	9.41
POS_17614	23.2671	760.5844	PC 34:1	C42H82NO8P	1.17	0.0253	7.64	5.52
POS_17444	22.8974	746.5686	PC 33:1	C41H80NO8P	1.42	0.0283	1.46	5.61
POS_17283	22.5208	734.5591	PC (14:0/18:0)	C40H80NO8P	1.39	0.0303	1.47	5.15

FIGURE 3 Phosphatidylcholine species predict CRT response. (A) Tuning parameter (λ) selection in the LASSO model used 10-fold cross-validation via minimum criteria. The binomial deviance was plotted versus log (λ). Dotted vertical lines were drawn at the optimal values by using minimum criteria and the 1 standard error (1-SE criteria). (B) LASSO coefficient profiles of the 20 features. A coefficient profile plot was produced against the log (λ) sequence. Dotted vertical line was drawn at the optimal λ at minimum criteria and 1 standard error (1-SE criteria). The model at 1-SE criteria was selected as the final model with four non-zero coefficients. (C) Boxplot (median and IQR) of four non-zero coefficients features between CRT responders and non-responders. (D) The area under curve (AUC) of receive operating characteristics (ROC) testing by combination of four selected features in training and testing dataset by cross validation under 500 random replications. (E) The ROC curves of four individual PCs metabolites and regression model incorporating four selected PCs in the whole CRT population (n = 42) showed that combination model had better discrimination (AUC = 0.906) for CRT response than individual PC metabolite. $^{***}P < 0.001$, $^{**}P < 0.01$.

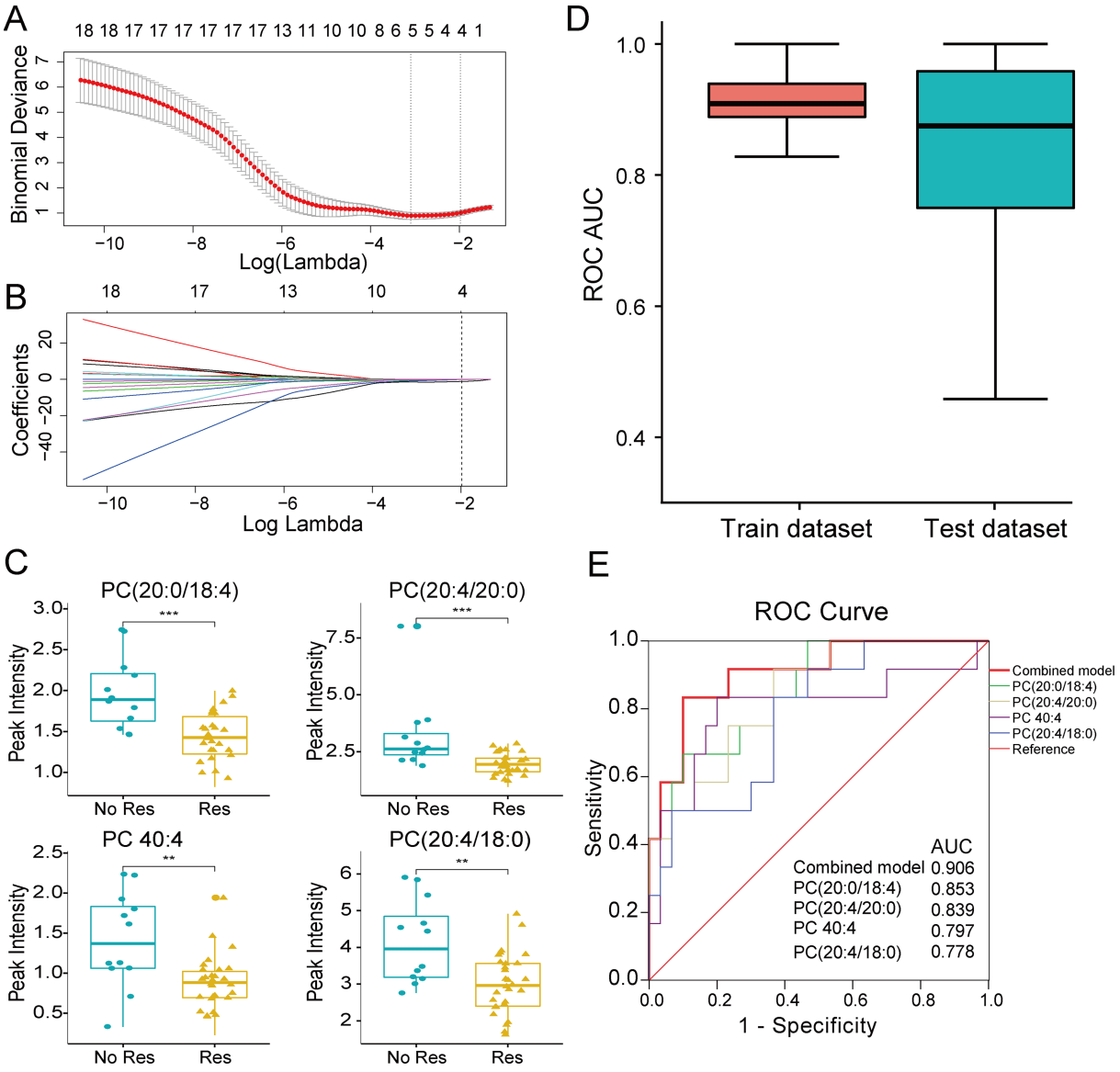

novel biomarkers and new potential targets for treatment. The human heart has unique metabolic flexibility and ability. It can switch the major source of energy to adapt to changing physiological or dietary conditions. Several studies have already demonstrated metabolomic profiles in patients with HF.[14,23–25] The main metabolic changes seen in a failing heart is the shift of energy utilization from fatty acids to glucose.[26] In the present study, compared with healthy individuals, we found that patients with HF had distinct metabolomic profiles, including increased long-chain free fatty acid, acylcarnitine, and ketone bodies. This finding is consistent with the previous studies.[15,24,27] Lipid species such as Cer and

SMs are important constituents of cell membranes and participate in several biological activities that may influence the pathophysiology of HF.[28,29] The relationship between Cer/SMs and the risk of HF has been identified.[30] In this study, we confirmed that Cer and SMs were different between HF patients and healthy controls as previously reported,[30,31] whereas we did not observe a significant difference in these metabolites between CRT responders and non-responders.

Based on the untargeted LC-MS/MS-based metabolomics analysis, we observed the significant differences in the ESI+ mode rather than ESI− mode between CRT responders and non-responders. This may be related to the different categories of substances detected by the metabolome positive (ESI +) and negative (ESI−) ion mode. In the positive ion mode, lipids such as PCs, Cer, plasmenyl-PCs, and SMs as well as amino acids are detected, whereas the negative ion mode metabolome contains long-chain fatty acid and amino acids, as well as lipids, such as FAHFA, PA, PE and phosphatidylethanolamine, but not containing PCs species. Between CRT non-responders and responders, the dominated differential metabolites were mainly PCs that were mostly upregulated in the plasma of CRT non-responders, compared with responders. Through LASSO regression, we further identified four metabolites among the 20 PCs. And the four PCs-based model displayed excellent performance for predicting CRT response outcome, with high specificity and sensitivity. Because this is a primary discovery study based on a small prospective cohort from a single centre, further validation is needed in multi-centre studies with larger cohorts.

In the present study, PCs species rather than various irrelevant metabolites were found as the distinct plasma metabolites between responders and non-responders to CRT, which is different from previous reports.[32,33] This may be related to changes in myocardial lipid homeostasis, especially PCs metabolism in the failing hearts.[34] As a common chronic disease, HF is associated with body consumption. With the development of HF, skeletal muscle loss occurs before fat tissue loss.[35,36] Furthermore, for patients with HF, plasma metabolomics not only represent the alteration in cardiac metabolism but also indicate overall metabolic changes in human body, because the circulating metabolites may involve the interaction between the heart and other organs. As a metabolic organ, the liver also plays an important role in the metabolism of PCs, and its abnormality may be related to the abnormal liver function of the failing heart.[24,37] PCs decomposition may be specifically affected as well during HF progression.

PCs are also key sources for the bioactive eicosanoids, which include leukotrienes, prostaglandins, and lipoxins. The enzyme phospholipases A2 (PLA2) is known to play an important role in the hydrolysis of phospholipids especially PCs, which leads to the accumulation of FFA including (non-esterified) arachidonic acid (AA).[38] As a free fatty acid, once being liberated from cell membranes in response to stimulation, AA can be metabolized to form bioactive products including PGs, leukotrienes, and epoxyeicosatrienoic acids, which participate in the inflammation process.[39] The amount of AA, as well as AA-containing PCs, depends on an exquisite balance between phospholipid reacylation and hydrolysis reactions.[40,41] Moon *et al.*[42] found that congestive HF is associated with the pathological opening of the mitochondrial permeability transition pore, which activates Ca^{2+}-independent phospholipase A2 (iPLA2) through decreasing the mitochondrial membrane potential. The activation of iPLA2 increased the production of downstream toxic hydroxyeicosatetraenoic acids. Of note, it is iPLA2, which activates AA into hydroxyeicosatetraenoic acids, rather than cPLA2, that predominated in failing human myocardium. In consistent with Moon's research, our study suggests the important value of AA-PCs in CRT response, indicating that the metabolism of AA and AA-PCs may play an important role in failing heart. In addition, disturbances and abnormal membrane phospholipids in the ratio of phosphatidylcholine to phosphatidylethanolamine in failing heart altered the interaction of membrane-associated protein complexes, thereby affecting the myocardial metabolism and cellular signalling.[43] Nevertheless, the mechanisms of potential correlation of cardiac lipid metabolism with response to CRT were rarely studied. Our novel findings, despite clinical association study, will provide a promising clue to study the potential pathophysiology of failing heart in response to CRT in the future. The potential mechanism between phosphatidylcholine metabolism and CRT responses still remain to be further illustrated in the future.

Study limitations

In this study, we used patients with an increase of LVEF more than 5% after CRT implantation as the definition of response to CRT. Thus, the performance using this panel to predict other definitions of responses to CRT is required. Moreover, the precise mechanisms association between PCs species and CRT response remains unclear, which should be explored in future studies. Additionally, the current study was performed in a single centre with a relatively small sample size. Multi-centre studies with larger populations as external validation groups are currently in progress by our team.

Conclusions

Heart failure is associated with a significantly altered metabolomics profile compared with healthy individuals. Within the HF group, the non-responders had a distinct plasma metabolic profile featuring alterations of 20 PC metabolites, compared with the responders to CRT. A novel predictive model incorporating four PCs performed well in identifying CRT

non-responders. These four PCs might severe as potential biomarkers for predicting CRT response. Further validation is needed in multi-centre studies with larger samples.

Conflict of interest

None declared.

Funding

This work was supported by the Chinese Academy of Medical Sciences Innovation Fund for Medical Sciences (2017-I2M-1-009) and the National Natural Science Foundation of China (81570370).

Supporting information

Additional supporting information may be found online in the Supporting Information section at the end of the article.

Table S1. Representative differential metabolites identified between heart failure patients and healthy controls.
Table S2. Ceramide and sphingomyelin species between CRT response and non-response patients

References

1. Benjamin EJ, Virani SS, Callaway CW, Chamberlain AM, Chang AR, Cheng S, Chiuve SE, Cushman M, Delling FN, Deo R, de Ferranti SD, Ferguson JF, Fornage M, Gillespie C, Isasi CR, Jiménez MC, Jordan LC, Judd SE, Lackland D, Lichtman JH, Lisabeth L, Liu S, Longenecker CT, Lutsey PL, Mackey JS, Matchar DB, Matsushita K, Mussolino ME, Nasir K, O'Flaherty M, Palaniappan LP, Pandey A, Pandey DK, Reeves MJ, Ritchey MD, Rodriguez CJ, Roth GA, Rosamond WD, Sampson UKA, Satou GM, Shah SH, Spartano NL, Tirschwell DL, Tsao CW, Voeks JH, Willey JZ, Wilkins JT, Wu JH, Alger HM, Wong SS, Muntner P, American Heart Association Council on Epidemiology and Prevention Statistics Committee and Stroke Statistics Subcommittee. Heart disease and stroke statistics-2018 update: a report from the American Heart Association. *Circulation* 2018; **137**: e67–e492.
2. Carley AN, Taegtmeyer H, Lewandowski ED. Matrix revisited: mechanisms linking energy substrate metabolism to the function of the heart. *Circ Res* 2014; **114**: 717–729.
3. Osterholt M, Sen S, Dilsizian V, Taegtmeyer H. Targeted metabolic imaging to improve the management of heart disease. *JACC Cardiovasc Imaging* 2012; **5**: 214–226.
4. Ventura-Clapier R, Garnier A, Veksler V. Energy metabolism in heart failure. *J Physiol* 2004; **555**: 1–13.
5. Bristow MR, Saxon LA, Boehmer J, Krueger S, Kass DA, De Marco T, Carson P, Di Carlo L, De Mets D, White BG, De Vries DW. Cardiac-resynchronization therapy with or without an implantable defibrillator in advanced chronic heart failure. *N Engl J Med* 2004; **350**: 2140–2150.
6. Cleland JG, Daubert JC, Erdmann E, Freemantle N, Gras D, Kappenberger L, Tavazzi L, Cardiac Resynchronization-Heart Failure (CARE-HF) Study Investigators. The effect of cardiac resynchronization on morbidity and mortality in heart failure. *N Engl J Med* 2005; **352**: 1539–1549.
7. Moss AJ, Hall WJ, Cannom DS, Klein H, Brown MW, Daubert JP, Estes NAM III, Foster E, Greenberg H, Higgins SL, Pfeffer MA, Solomon SD, Wilber D, Zareba W. Cardiac-resynchronization therapy for the prevention of heart-failure events. *N Engl J Med* 2009; **361**: 1329–1338.
8. Tang AS, Wells GA, Talajic M, Arnold MO, Sheldon R, Connolly S, Hohnloser SH, Nichol G, Birnie DH, Sapp JL, Yee R, Healey JS, Rouleau JL, Resynchronization-Defibrillation for Ambulatory Heart Failure Trial Investigators. Cardiac-resynchronization therapy for mild-to-moderate heart failure. *N Engl J Med* 2010; **363**: 2385–2395.
9. Linde C, Abraham WT, Gold MR, St John Sutton M, Ghio S, Daubert C, REVERSE (REsynchronization reVErses Remodeling in Systolic left vEntricular dysfunction) Study Group. Randomized trial of cardiac resynchronization in mildly symptomatic heart failure patients and in asymptomatic patients with left ventricular dysfunction and previous heart failure symptoms. *J Am Coll Cardiol* 2008; **52**: 1834–1843.
10. McAlister FA, Ezekowitz J, Hooton N, Vandermeer B, Spooner C, Dryden DM, Page RL, Hlatky MA, Rowe BH. Cardiac resynchronization therapy for patients with left ventricular systolic dysfunction: a systematic review. *JAMA* 2007; **297**: 2502–2514.
11. Chung ES, Leon AR, Tavazzi L, Sun JP, Nihoyannopoulos P, Merlino J, Abraham WT, Ghio S, Leclercq C, Bax JJ, Yu CM, Gorcsan J III, St John Sutton M, de Sutter J, Murillo J. Results of the predictors of response to CRT (PROSPECT) trial. *Circulation* 2008; **117**: 2608–2616.
12. Zamboni N, Saghatelian A, Patti GJ. Defining the metabolome: size, flux, and regulation. *Mol Cell* 2015; **58**: 699–706.
13. Trivedi DK, Hollywood KA, Goodacre R. Metabolomics for the masses: the future of metabolomics in a personalized world. *New Horiz Transl Med* 2017; **3**: 294–305.
14. Stenemo M, Ganna A, Salihovic S, Nowak C, Sundstrom J, Giedraitis V, Broeckling CD, Prenni JE, Svensson P, Magnusson PK, Lind L. The metabolites urobilin and sphingomyelin (30:1) are associated with incident heart failure in the general population. *ESC Heart Fail* 2019; **6**: 764–773.
15. Lanfear DE, Gibbs JJ, Li J, She R, Petucci C, Culver JA, Tang WHW, Pinto YM, Williams LK, Sabbah HN, Gardell SJ. Targeted metabolomic profiling of plasma and survival in heart failure patients. *JACC Heart Fail* 2017; **5**: 823–832.
16. Brignole M, Auricchio A, Baron-Esquivias G, Bordachar P, Boriani G, Breithardt OA, Cleland J, Deharo JC, Delgado V, Elliott PM. 2013 ESC guidelines on cardiac pacing and cardiac resynchronization therapy: The Task Force on cardiac pacing and resynchronization therapy of the European Society of Cardiology (ESC). Developed in collaboration with the European Heart Rhythm Association (EHRA). *Eur Heart J* 2013; **34**: 2281–2329.
17. Lang RM, Badano LP, Mor-Avi V, Afilalo J, Armstrong A, Ernande L, Flachskampf FA, Foster E, Goldstein SA, Kuznetsova T, Lancellotti P, Muraru D, Picard MH,

Rietzschel ER, Rudski L, Spencer KT, Tsang W, Voigt JU. Recommendations for cardiac chamber quantification by echocardiography in adults: an update from the American Society of Echocardiography and the European Association of Cardiovascular Imaging. *Eur Heart J Cardiovasc Imaging* 2015; **16**: 233–270.
18. Blumenthal RS, Becker DM, Yanek LR, Moy TF, Michos ED, Fishman EK, Becker LC. Comparison of coronary calcium and stress myocardial perfusion imaging in apparently healthy siblings of individuals with premature coronary artery disease. *Am J Cardiol* 2006; **97**: 328–333.
19. Bax JJ, Marwick TH, Molhoek SG, Bleeker GB, van Erven L, Boersma E, Steendijk P, van der Wall EE, Schalij MJ. Left ventricular dyssynchrony predicts benefit of cardiac resynchronization therapy in patients with end-stage heart failure before pacemaker implantation. *Am J Cardiol* 2003; **92**: 1238–1240.
20. Zweerink A, van Everdingen WM, Nijveldt R, Salden OAE, Meine M, Maass AH, Vernooy K, de Lange FJ, Vos MA, Croisille P, Clarysse P, Geelhoed B, Rienstra M, van Gelder IC, van Rossum AC, Cramer MJ, Allaart CP. Strain imaging to predict response to cardiac resynchronization therapy: a systematic comparison of strain parameters using multiple imaging techniques. *ESC Heart Fail* 2018; **5**: 1130–1140.
21. Yang S, Liu Z, Liu S, Ding L, Chen K, Hua W, Zhang S. Association of baseline big endothelin-1 level with long-term prognosis among cardiac resynchronization therapy recipients. *Clin Biochem* 2018; **59**: 25–30.
22. Hsu JC, Solomon SD, Bourgoun M, McNitt S, Goldenberg I, Klein H, Moss AJ, Foster E. Predictors of super-response to cardiac resynchronization therapy and associated improvement in clinical outcome: the MADIT-CRT (multicenter automatic defibrillator implantation trial with cardiac resynchronization therapy) study. *J Am Coll Cardiol* 2012; **59**: 2366–2373.
23. Ahmad T, Kelly JP, McGarrah RW, Hellkamp AS, Fiuzat M, Testani JM, Wang TS, Verma A, Samsky MD, Donahue MP, Ilkayeva OR. Prognostic implications of long-chain acylcarnitines in heart failure and reversibility with mechanical circulatory support. *J Am Coll Cardiol* 2016; **67**: 291–299.
24. Cheng ML, Wang CH, Shiao MS, Liu MH, Huang YY, Huang CY, Mao CT, Lin JF, Ho HY, Yang NI. Metabolic disturbances identified in plasma are associated with outcomes in patients with heart failure: diagnostic and prognostic value of metabolomics. *J Am Coll Cardiol* 2015; **65**: 1509–1520.
25. Yoshihisa A, Watanabe S, Yokokawa T, Misaka T, Sato T, Suzuki S, Oikawa M, Kobayashi A, Takeishi Y. Associations between acylcarnitine to free carnitine ratio and adverse prognosis in heart failure patients with reduced or preserved ejection fraction. *ESC Heart Fail* 2017; **4**: 360–364.
26. Gupta A, Houston B. A comprehensive review of the bioenergetics of fatty acid and glucose metabolism in the healthy and failing heart in nondiabetic condition. *Heart Fail Rev* 2017; **22**: 825–842.
27. Albert CL, Tang WHW. Metabolic biomarkers in heart failure. *Heart Fail Clin* 2018; **14**: 109–118.
28. Kolter T. A view on sphingolipids and disease. *Chem Phys Lipids* 2011; **164**: 590–606.
29. Jiang XC, Goldberg IJ, Park TS. Sphingolipids and cardiovascular diseases: lipoprotein metabolism, atherosclerosis and cardiomyopathy. *Adv Exp Med Biol* 2011; **721**: 19–39.
30. Lemaitre RN, Jensen PN, Hoofnagle A, McKnight B, Fretts AM, King IB, Siscovick DS, Psaty BM, Heckbert SR, Mozaffarian D, Sotoodehnia N. Plasma ceramides and sphingomyelins in relation to heart failure risk. *Circ Heart Fail* 2019; **12**: e005708.
31. Hilvo M, Meikle PJ, Pedersen ER, Tell GS, Dhar I, Brenner H, Schöttker B, Lääperi M, Kauhanen D, Koistinen KM, Jylhä A, Huynh K, Mellett NA, Tonkin AM, Sullivan DR, Simes J, Nestel P, Koenig W, Rothenbacher D, Nygård O, Laaksonen R. Development and validation of a ceramide- and phospholipid-based cardiovascular risk estimation score for coronary artery disease patients. *Eur Heart J* 2020; **41**: 371–380.
32. Mueller-Hennessen M, Dungen HD, Lutz M, Trippel TD, Kreuter M, Sigl J, Müller OJ, Tahirovic E, Witt H, Ternes P, Carvalho S. A novel lipid biomarker panel for the detection of heart failure with reduced ejection fraction. *Clin Chem* 2017; **63**: 267–277.
33. Marcinkiewicz-Siemion M, Ciborowski M, Ptaszynska-Kopczynska K, Szpakowicz A, Lisowska A, Jasiewicz M, Waszkiewicz E, Kretowski A, Musial WJ, Kaminski KA. LC-MS-based serum fingerprinting reveals significant dysregulation of phospholipids in chronic heart failure. *J Pharm Biomed Anal* 2018; **154**: 354–363.
34. Wende AR, Abel ED. Lipotoxicity in the heart. *Biochim Biophys Acta* 2010; **1801**: 311–319.
35. von Haehling S. The wasting continuum in heart failure: from sarcopenia to cachexia. *Proc Nutr Soc* 2015; **74**: 367–377.
36. von Haehling S, Ebner N, Dos Santos MR, Springer J, Anker SD. Muscle wasting and cachexia in heart failure: mechanisms and therapies. *Nat Rev Cardiol* 2017; **14**: 323–341.
37. Ming YN, Zhang JY, Wang XL, Li CM, Ma SC, Wang ZY, Liu XL, Li XB, Mao YM. Liquid chromatography mass spectrometry-based profiling of phosphatidylcholine and phosphatidylethanolamine in the plasma and liver of acetaminophen-induced liver injured mice. *Lipids Health Dis* 2017; **16**: 153.
38. Zhang LX, Liu ZY. Effects of microiontophoretically applied ACH and atropine on the electric activities of neurons in nucleus parafascicularis of thalamus in rats. *Sheng Li Xue Bao* 1993; **45**: 55–60.
39. Hanna VS, Hafez EAA. Synopsis of arachidonic acid metabolism: a review. *J Adv Res* 2018; **11**: 23–32.
40. Perez-Chacon G, Astudillo AM, Balgoma D, Balboa MA, Balsinde J. Control of free arachidonic acid levels by phospholipases A2 and lysophospholipid acyltransferases. *Biochim Biophys Acta* 1791; **2009**: 1103–1113.
41. Stables MJ, Gilroy DW. Old and new generation lipid mediators in acute inflammation and resolution. *Prog Lipid Res* 2011; **50**: 35–51.
42. Moon SH, Liu X, Cedars AM, Yang K, Kiebish MA, Joseph SM, Kelley J, Jenkins CM, Gross RW. Heart failure-induced activation of phospholipase iPLA2γ generates hydroxyeicosatetraenoic acids opening the mitochondrial permeability transition pore. *J Biol Chem* 2018; **293**: 115–129.
43. Frangogiannis NG. The extracellular matrix in myocardial injury, repair, and remodeling. *J Clin Invest* 2017; **127**: 1600–1612.